Synchronized Independent Narrow-Band Single Photons and Efficient Generation of Photonic Entanglement

Zhen-Sheng Yuan,[1,2] Yu-Ao Chen,[1] Shuai Chen,[1] Bo Zhao,[1] Markus Koch,[1] Thorsten Strassel,[1] Yong Zhao,[1] Gan-Jun Zhu,[1] Jörg Schmiedmayer,[1,3] and Jian-Wei Pan[1,2]

[1]*Physikalisches Institut, Ruprecht-Karls-Universität Heidelberg, Philosophenweg 12, 69120 Heidelberg, Germany*
[2]*Hefei National Laboratory for Physical Sciences at Microscale and Department of Modern Physics, University of Science and Technology of China, Hefei, Anhui 230026, China*
[3]*Atominstitut der österreichischen Universitäten, TU-Wien, A-1020 Vienna Austria*

(Received 20 March 2007; published 4 May 2007)

We create independent, synchronized single-photon sources with built-in quantum memory based on two remote cold atomic ensembles. The synchronized single photons are used to demonstrate efficient generation of entanglement. The resulting entangled photon pairs violate a Bell's inequality by 5 standard deviations. Our synchronized single photons with their long coherence time of 25 ns and the efficient creation of entanglement serve as an ideal building block for scalable linear optical quantum information processing.

DOI: 10.1103/PhysRevLett.98.180503 PACS numbers: 03.67.Hk, 32.80.Pj, 42.50.Dv

Synchronized generation of either deterministic and storable single photons or entangled photon pairs is essential for scalable linear optical quantum information processing (LOQIP). With the help of quantum memory and feed-forward, one can thus achieve long-distance quantum communication [1–3] and efficient quantum computation [4–7]. Very recently, interfering synchronized independent single photons [8] and entangled photon pairs [9] have been experimentally achieved with two pulsed spontaneous parametric down-conversion sources pumped by two synchronized but mutually incoherent femto-second lasers. However, due to the absence of quantum memory for broadband (a few nm) single photons, no feedback was applied in the above experiments; single photons or entangled photon pairs were merely generated probabilistically in each experimental run, i.e., with a small probability p. Thus, in an experiment concerning manipulation of N synchronized single (or entangled) photon sources, the experimental efficiency will decrease exponentially with the number of sources (proportional to p^N). Moreover, the short coherence time of down-converted photons ($\sim$ a few hundred fs, defined by the bandwidth of interference filters) also makes hard the overlap of photon wave packets coming from two distant sites. These two drawbacks together make the above experiments inappropriate for scalable LOQIP.

Following a recent proposal for long-distance quantum communication with atomic ensembles [3] (see also the improved schemes [10]), it is possible to generate narrow-band single photons or entangled photon pairs in a deterministic and storable fashion. In the past years, significant experimental progresses have been achieved in demonstration of quantum storage and single-photon sources [11,12], and even entanglement in number basis for two atomic ensembles has been demonstrated experimentally [13]. Moreover, deterministic narrow-band single-photon sources have been demonstrated most recently with the help of quantum memory and electronic feedback circuits [14–16].

In this Letter, we develop further the techniques used in Ref. [14] to implement synchronized generation of two independent single-photon sources from two remote atomic ensembles loaded by magneto-optical traps (MOT). The two synchronized single photons are further used to demonstrate efficient generation of entangled photon pairs. Since our single-photon sources are generated in-principle in a deterministic and storable fashion, with the help of feed-forward the experimental methods can be used for scalable generation of photonic entanglement. Moreover, compared to the short coherence time of down-converted photons in Refs. [8,9], the coherence time of our synchronized narrow-band single photons is about 25 ns, four orders longer, which makes it much easier to overlap independent photon wave packets from distant sites for further applications of LOQIP. Finally, it is worth noting that the read and write lasers used for different single-photon sources are fully independent to each other. The synchronization was achieved by separate electronic signals generated by the control electronics.

The basic concept of our experiment is illustrated in Fig. 1. Atomic ensembles collected by two MOT's 0.6 m apart function as the media for quantum memories and deterministic single-photon sources. Each ensemble consists of about 10^8 ^{87}Rb atoms. The two hyperfine ground states $|5S_{1/2}, F = 2\rangle = |a\rangle$ and $|5S_{1/2}, F = 1\rangle = |b\rangle$ and the excited state $|5P_{1/2}, F = 2\rangle = |e\rangle$ form a Λ-type system $|a\rangle - |e\rangle - |b\rangle$. The atoms are initially optically pumped to state $|a\rangle$. Shining a weak classical *write* pulse with the Rabi frequency Ω_W into the atoms creates a superposed state of the anti-Stokes field $\hat{a}_{\mathrm{AS}}$ and a collective spin state of the atoms,

$$|\Psi\rangle \sim |0_{\mathrm{AS}}0_b\rangle + \sqrt{\chi}|1_{\mathrm{AS}}1_b\rangle + \chi|2_{\mathrm{AS}}2_b\rangle + O(\chi^{3/2}), \quad (1)$$

where $\chi \ll 1$ is the excitation probability of one spin flip,

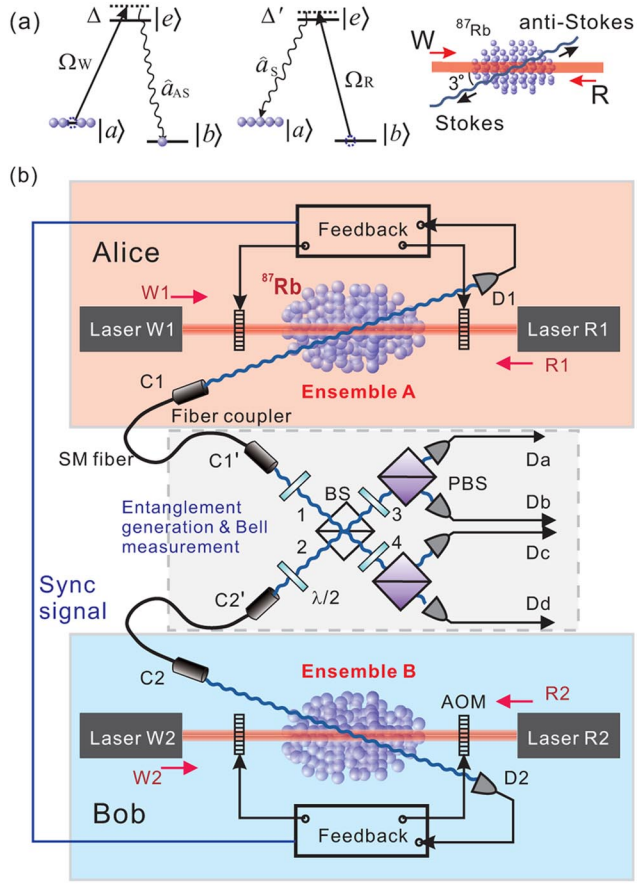

FIG. 1 (color online). Illustration of the relevant energy levels of the atoms and arrangement of laser beams (a) and the experimental setup (b). (a) ^{87}Rb atoms are prepared in the initial state $|a\rangle$. A write pulse Ω_W with the detuning of $\Delta = 10$ MHz and a beam diameter about 400 μm is applied to generate the spin excitation and an accompanying photon of the anti-Stokes field $\hat{a}_{\mathrm{AS}}$ with a beam diameter about 100 μm. The mode $\hat{a}_{\mathrm{AS}}$, tilted 3° from the direction of the write beam, is coupled in a single-mode fiber (SMF) and guided to a single-photon detector. Waiting for a duration δt_R, a read pulse is applied with orthogonal polarization and spatially mode-matched with the write beam from the opposite direction. The spin excitation in the atomic ensemble will be retrieved into a single photon of the Stokes field $\hat{a}_S$, which propagates to the opposite direction of the field $\hat{a}_{\mathrm{AS}}$ and is also coupled in SMF. (b) Alice and Bob each keeps a single-photon source at two remote locations. As elucidated in Ref. [14], Alice applies write pulses continuously until an anti-Stokes photon is registered by detector D1. Then she stops the write pulse, holds the spin excitations, and meanwhile sends a synchronization signal to Bob and waits for his response. (This is realized by the feedback circuit and the acousto-optic modulators, AOM.) In parallel, Bob prepares a single excitation in the same way as Alice. After they both agree that each has a spin excitation, each of them will apply a read pulse simultaneously to retrieve the spin excitation into a light field $\hat{a}_S$. The two Stokes photons propagate to the place for entanglement generation and Bell measurement. They overlap at a 50:50 beam splitter (BS) and then will be analyzed by latter half wave plates ($\lambda/2$), polarized beam splitters (PBS) and single-photon detectors Da, Db, Dc, and Dd.

and $|i_{\mathrm{AS}} i_b\rangle$ denotes the i-fold excitation of the anti-Stokes field and the collective spin. Ideally, conditioned on detecting one and only one anti-Stokes photon, a single spin excitation is generated in the atomic ensemble with certainty. In practice, considering photon loss in the detection, this condition can be fulfilled by keeping $\chi \ll 1$ so as to make the multi excitations negligibly small. After a controllable time delay δt_R (in the order of the lifetime τ_c of the spin excitation), another classical *read* pulse with the Rabi frequency Ω_R is applied to retrieve the spin excitation and generate a photon in the Stokes field $\hat{a}_S$. If the retrieve efficiency reaches unity, the Stokes photon is no longer probabilistic because of the quantum memory and feedback control [14–16], which now can serve as a deterministic single-photon source. As shown in Fig. 1, Alice and Bob both have such a source. They prepare collective spin excitations independently, and the one who finishes the preparation first will wait for the other while keeping the collective spin excitation in his or her quantum memory. After they agree that both have finished the preparation, they retrieve the excitations simultaneously at any time they want within the lifetime of the collective state. Therefore, the retrieved photons arrive at the beam splitter with the required timing.

Compared to a probabilistic photon source, the present implementation with atomic ensembles contributes a considerable enhancement to the coincidence rate of single photons coming from Alice and Bob. For instance, we consider a similar setup but without feedback circuit, where Alice and Bob apply write and read in every experimental trial and thereafter measure the fourfold coincidence of anti-Stokes and Stokes photons in the four channels D1, D2, C1, and C2. Assume the probability to have an anti-Stokes photon in channel D1 (D2) is p_{AS1} (p_{AS2}) and the corresponding retrieve efficiency for conversion of the spin excitation to a Stokes photon coupled into channel C1 (C2) is $\gamma_1(\delta t_R)$ [$\gamma_2(\delta t_R)$], then the probability of fourfold coincidence is $p_{4c} = p_{\mathrm{AS1}}\gamma_1(\delta t_R) \times p_{\mathrm{AS2}}\gamma_2(\delta t_R)$. This has to be compared with using the feedback circuits shown in Fig. 1, where we can apply at most N (limited by the lifetime of the quantum memory and the speed of the feedback circuit) write pulses in each trial. Then the probability of fourfold coincidence becomes

$$P_{4c} = \Bigg\{ \sum_{i=0}^{N-1} p_{\mathrm{AS1}}(1 - p_{\mathrm{AS1}})^i \times \sum_{j=i}^{N-1} p_{\mathrm{AS2}}(1 - p_{\mathrm{AS2}})^j \gamma_2(\delta t_R) \times \gamma_1[(j-i)\delta t_W + \delta t_R] \Bigg\} + \{\cdots\}_{1\leftrightarrow 2}, \quad (2)$$

where δt_W is the time interval between the sequential write pulses [14] and $\{\cdots\}_{1\leftrightarrow 2}$ is the same as the first term with index 1 and 2 being exchanged. Assume $p_{\mathrm{AS1}} \ll 1$ and $p_{\mathrm{AS2}} \ll 1$ and a long lifetime τ_c, we obtain

$P_{4c} \sim N^2 p_{\mathrm{AS1}}\gamma_1(\delta t_R) p_{\mathrm{AS2}}\gamma_2(\delta t_R)$ for a definite number N. So the probability of fourfold coincidence is enhanced by N^2 for each trial. For our case, $p_{\mathrm{AS1}} \approx p_{\mathrm{AS2}} = 2.0 \times 10^{-3}$ (the relevant cross correlation $g^{(2)}_{\mathrm{AS},S} = 30$), $N = 12$, $\tau_c \sim 12\ \mu$s, $\delta t_W = 800$ ns, $\delta t_R = 400$ ns, and $\gamma_1(0) \approx \gamma_2(0) = 8\%$, the enhancement is 136.

The four lasers in Fig. 1 are independently frequency stabilized. The linewidths of $W1$ and $R1$ are about 1 MHz while those of $W2$ and $R2$ are about 5 MHz of the full width at half maximum (FWHM). However, they will be broadened to more than 20 MHz because the laser pulse modulated by the AOM is a Gaussian-like profile with width about 40 ns FWHM. The linewidth of the retrieved single photons is determined mainly by the linewidth and intensity of the read lasers. So we try to make the profile of the two independent read pulses identical to each other.

In order to verify that the two Stokes photons coming from Alice and Bob are indistinguishable, we let them overlap at a BS with the same polarization (horizontal in our case) and measure the quantum interference indicated by the the Hong-Ou-Mandel (HOM) dip [17]. Having observed the high visibility of HOM dip in both time domain and frequency domain, we are confirmed that the two independent photons are indistinguishable. Then we put one of the two photons to vertical polarized before they enter the BS. By coincidence measurement at the two outputs of the BS, we generate the Bell state $|\Psi^-\rangle_{12} = \frac{1}{\sqrt{2}}(|H\rangle_1|V\rangle_2 - |V\rangle_1|H\rangle_2)$, which is verified by the measurement of violation of Bell's inequality.

The measurement of HOM dip.—We did two measurements to obtain the HOM dip in time domain and frequency domain, respectively. To make the photons indistinguishable, the polarizations of the anti-Stokes photons were set to horizontal with two half-wave plates before they enter the BS as shown in Fig. 1. The other two half-wave plates after the BS were set to 0°.

In the first measurement, we measured the fourfold coincidence among detectors D1, D2, Da, and Dd while changing the time delay between the two read pulses (Fig. 2, left panel). The excitation probabilities $p_{\mathrm{AS1}} \approx p_{\mathrm{AS2}} = 2.0 \times 10^{-3}$. The coincidence rate is varied with the delay. Ideally, there should be completely destructive interference if the wave packets of the two photons overlap perfectly. However, it is hard to make the two wave packets absolutely identical or exactly overlapped in practice. We obtained the visibility of the dip $V = (C_{\mathrm{plat}} - C_{\mathrm{dip}})/C_{\mathrm{plat}} = (80 \pm 1)\%$, where C_{plat} is the noncorrelated coincidence rate at the plateau and C_{dip} is the interfering coincidence rate at the dip. The asymmetry of the profile at negative delay and positive delay shows that the two wave packets are (a) not perfectly identical, (b) not symmetric themselves. Assume the HOM dip is a Gaussian-type profile, we estimate the coherence time is 25 ± 1 ns FWHM.

In the second measurement, we measured the fourfold coincidence among detectors D1, D2, Da, and Dd while changing the frequency detuning between the two read pulses (Fig. 2, right panel). It is the first time to measure HOM dip in frequency domain at single-photon level. The excitation probabilities are $p_{\mathrm{AS1}} \approx p_{\mathrm{AS2}} = 3.0 \times 10^{-3}$, higher than those in time domain. Because of the limit of the current setup, the detuning can be varied from -30 MHz to 30 MHz. In order to verify the coincidence rate at largest detuning reached the plateau of HOM dip, we measured the coincidence by setting the polarization of the two photons perpendicular to each other and zero detuning between the two read lasers (shown as a circle in Fig. 2). The consistence of this data with those two at largest detunings shows that we have achieved the plateau of HOM dip. The visibility is $(82 \pm 3)\%$ which agrees well with that obtained in time domain. The width of the HOM dip is 35 ± 3 MHz FWHM, in accordance with the coherence time 25 ns. Therefore, the narrow-band characteristic of the present source is verified directly by the HOM dip in the frequency domain.

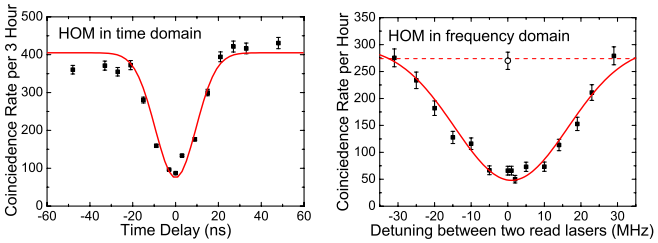

FIG. 2 (color online). Hong-Ou-Mandel dips in time domain (left panel) and frequency domain (right panel). The circle in the right panel was obtained by setting the polarization of the two photons perpendicular to each other and zero detuning between two read lasers. The Gaussian curves that roughly connect the data points are only shown to guide the eye. The dashed line shows the plateau of the dip. Error bars represent statistical errors, which are $\pm$ 1 standard deviation.

Besides the imperfect overlap of the single-photon wave packets, the two-photon components in each of the single-photon sources affect the visibility as well. The quality of single-photon source is characterized by the anticorrelation parameter $\alpha = 2P_{\mathrm{II}}/P_{\mathrm{I}}^2$ [14], where P_{I} (P_{II}) is the probability of generating one (two) photon(s) for each source (the higher orders are negligible small). If the two wave packets do not overlap at all, there is no interference between them. Then we obtain the noncorrelated coincidence rate $C_{\mathrm{plat}} = P_{\mathrm{I}}^2/2 + P_{\mathrm{II}}$ between Da and Dd. If they overlap perfectly, there is destructive interference leading to a coincidence rate $C_{\mathrm{dip}} = P_{\mathrm{II}}$. So the visibility of the HOM dip is $V = 1/(1 + \alpha)$. In our experiment, $\alpha = 0.12$ for the source prepared later (the spin excitation is retrieved immediately) and $\alpha = 0.17$ for the source prepared earlier (it has to wait for the other one). This leads to an average visibility of 87%. In the frequency domain, the average visibility is around 83% because of higher excitation probabilities.

TABLE I. Correlation functions E and the resulting S.

E	$\theta_1 = 0°$	$\theta_1' = 45°$	S
$\theta_2 = 22.5°$	-0.613 ± 0.037	0.575 ± 0.039	
$\theta_2' = -22.5°$	0.606 ± 0.038	0.579 ± 0.039	2.37 ± 0.07

Efficient entanglement generation.—As shown in Fig. 1, we set orthogonal polarizations (horizontal and vertical) of the Stokes photons with the two half wave plates before the BS. Then the state of the two photons will be projected to $|\Psi^-\rangle_{12}$ if there is coincidence between the two output ports 3 and 4. With another two half wave plates and two PBS after the BS, the entanglement of the two photons can be verified by a Clauser-Horne-Shimony-Holt (CHSH) type inequality [18], where $S \leq 2$ for any local realistic theory with

$$S = |E(\theta_1, \theta_2) - E(\theta_1, \theta_2') - E(\theta_1', \theta_2) - E(\theta_1', \theta_2')|. \quad (3)$$

Here $E(\theta_1, \theta_2)$ is the correlation function where θ_1 and θ_1' (θ_2 and θ_2') are the measured polarization angles of the Stokes photon at port 3 (4). The observed values of the correlation functions are listed in Table I resulting in $S = 2.37 \pm 0.07$, which violates Bell's inequality by 5 standard deviations. This clearly confirms the quantum nature of the entanglement state.

With our imperfect sources, we do not create a perfect $|\Psi^-\rangle_{12}$. If we consider the two-photon component in the photon sources, the created state will be

$$|\Psi_{\text{eff}}\rangle_{12} = \begin{cases} P_{\text{I}}^2/2,\ 1/\sqrt{2}(|H\rangle_1|V\rangle_2 - |V\rangle_1|H\rangle_2); \\ P_{\text{II}}/2,\ |H\rangle_1|H\rangle_2; \\ P_{\text{II}}/2,\ |V\rangle_1|V\rangle_2. \end{cases} \quad (4)$$

From the quality of the single photons generated from the two ensembles, $\alpha = 0.12$, 0.17, and Eq. (4), we estimate the expected violation of Bell's inequality is around 2.3, which is in good agreement with our measured value. It is interesting to note that a violation of Bell's inequality needs a single-photon source with $\alpha < 0.24$ according to Eq. (4). In order to minimize α, further improvements, e.g., a higher optical couple efficiency, a lower photon loss, a lower excitation probability, and a higher retrieve efficiency, will be made in our future investigations.

In conclusion, we realized synchronized generation of narrow-band single photons with two remote atomic ensembles. The Hong-Ou-Mandel dip was observed in both time domain and frequency domain with a high visibility for independent photons coming from two distant sites, which shows the indistinguishability of these photons. By virtue of quantum memories and feedback circuits, the efficiency of generating entangled photon pairs was enhanced by a factor of 136, which claims our single-photon source as a promising candidate for the future implementation of scalable quantum computation based on linear optics [4–7]. The present spatially-distributed independent single-photon sources (with fully independent write and read lasers) are prerequirements for the long-distance quantum communication [1,10]. The narrow-band property (which makes the overlap of the photon wave packets at the order of nanoseconds) of single photons and high efficiency of entanglement generation also profit the present source to serve as an ideal candidate for large scale communications, e.g., satellite-based quantum communication. There is still potential to improve our single-photon source. We can improve the retrieve efficiency close to unity by increasing the optical density of the atomic ensemble. A better compensation of the stray magnetic field will help the extension of the lifetime up to 100 μs. If we want an even longer lifetime, a good solution is to confine the atoms in an optical trap, which also benefits to a much higher optical density.

This work was supported by the Deutsche Forschungsgemeinschaft (DFG), the Alexander von Humboldt Foundation, the Deutsche Telekom Stiftung, the Konrad-Adenauer Stiftung, the LGFG, and the CAS.

Note added.—During the final phases of our experiment, we became aware of two related experiments [19,20].

[1] H.-J. Briegel, W. Dür, J. I. Cirac, and P. Zoller, Phys. Rev. Lett. **81**, 5932 (1998).
[2] J.-W. Pan, C. Simon, Časlav Brukner, and A. Zeilinger, Nature (London) **410**, 1067 (2001).
[3] L.-M. Duan, M. D. Lukin, J. I. Cirac, and P. Zoller, Nature (London) **414**, 413 (2001).
[4] E. Knill, R. Laflamme, and G. J. Milburn, Nature (London) **409**, 46 (2001).
[5] R. Raussendorf and H. J. Briegel, Phys. Rev. Lett. **86**, 5188 (2001).
[6] M. A. Nielsen, Phys. Rev. Lett. **93**, 040503 (2004).
[7] D. E. Browne and T. Rudolph, Phys. Rev. Lett. **95**, 010501 (2005).
[8] R. Kaltenbaek *et al.*, Phys. Rev. Lett. **96**, 240502 (2006).
[9] T. Yang *et al.*, Phys. Rev. Lett. **96**, 110501 (2006).
[10] Z.-B. Chen, B. Zhao, J. Schmiedmayer, and J.-W. Pan, arXiv:quant-ph/0609151; B. Zhao *et al.*, arXiv:quant-ph/0609154); L. Jiang, J. M. Taylor, and M. D. Lukin, arXiv:quant-ph/0609236.
[11] T. Chanelière *et al.*, Nature (London) **438**, 833 (2005).
[12] M. D. Eisaman *et al.*, Nature (London) **438**, 837 (2005).
[13] C. W. Chou *et al.*, Nature (London) **438**, 828 (2005).
[14] S. Chen *et al.*, Phys. Rev. Lett. **97**, 173004 (2006).
[15] H. de Riedmatten *et al.*, Phys. Rev. Lett. **97**, 113603 (2006).
[16] D. N. Matsukevich *et al.*, Phys. Rev. Lett. **97**, 013601 (2006).
[17] C. K. Hong, Z. Y. Ou, and L. Mandel, Phys. Rev. Lett. **59**, 2044 (1987).
[18] J. F. Clauser, M. Horne, A. Shimony, and R. A. Holt, Phys. Rev. Lett. **23**, 880 (1969).
[19] D. Felinto *et al.*, Nature Phys. **2**, 844 (2006).
[20] T. Chanelière *et al.*, Phys. Rev. Lett. **98**, 113602 (2007).